Jurnal Teknologi

Full paper

Flame and Emission Characteristics of a Premixed Swirl-stabilised Burner

Chen Wei Kew[a], Cheng Tung Chong[a*], Jo-Han Ng[b,c], Boon Tuan Tee[d], Mohamad Nazri Mohd Jaafar[a]

[a]*Faculty of Mechanical Engineering, Universiti Teknologi Malaysia, 81310 UTM Johor Bahru, Johor Malaysia*
[b]*Faculty of Engineering and the Environment, University of Southampton, Malaysia Campus (USMC), 79200 Nusajaya, Johor, Malaysia*
[c]*Energy Technology Research Group, Highfield Campus, University of Southampton, Southampton, S017 1BJ, United Kingdom*
[d]*Department of Thermal Fluids, Faculty of Mechanical Engineering, Universiti Teknikal Malaysia Melaka, Melaka, Malaysia*

*Corresponding author: ctchong@mail.fkm.utm.my

Article history

Received 2 January 2014
Received in revised form 15 July 2014
Accepted 24 August 2014

Graphical abstract

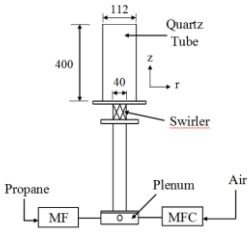

Abstract

The flame and emission characteristics of a premixed gaseous flame swirl burner are investigated under various equivalence ratio. The swirl flame is established using propane/air mixture at atmospheric condition. Flame imaging was performed to compare the global flame shape and intensity over a range of equivalence ratios and flow rates. Fuel-rich flame shows increased intensity due to the presence of soot formation. The lean blowout test was performed to determine the operating limit of the burner. Emissions of the propane swirl flame were measured at the exit of the burner outlet. Results show that NO_x emissions peak at stoichiometric condition, ϕ =1 as compared to the lean- and rich-burning regions. Carbon monoxide (CO) and unburned hydrocarbons (UHC) emissions were found to be low (< 10 ppm) under premixed, continuous swirl burning conditions for the equivalence ratio range of ϕ = 0.7-1.1.

Keywords: propane; swirl; burner; emissions; NO_x

1.0 INTRODUCTION

The use of combustion devices require detailed characterisation of performance and emissions to ensure the least impact to the environment. In many combustion devices, swirling flames are utilised to enhance fuel/air mixing, increase flame burning intensity and stabilize flame [1-3]. Substantial research has been focusing on the influence of swirl on flame stability, combustion efficiency as well as emissions performance.

Emissions measurements using swirl combustor of different configurations have been performed by various groups. Khalil and Gupta [4] measured the emissions of gaseous and liquid fuels using a fuel-flexible swirl combustor. Chong and Hochgreb utilised an axial swirl burner to investigate the flow field [5] and emissions of liquid swirl flames [6-8]. Nemitallah and Habib [9] investigated the oxy-combustion flame in diffusional mode and characterised the emissions using a swirl burner. The fuel used was methane and the oxidizer consists of a carbon monoxide (CO) and oxygen (O_2) mixture. Kim *et al.* [10] measured the emissions of hydrogen-added methane flames. Hydrogen was added to the methane-air mixture in the range of 2-9%. It was reported that the CO concentration is lower for hydrogen enriched flames due to lower carbon content and high combustibility of the hydrogen enriched fuel. The CO emissions were higher at lower adiabatic temperature because of deficiency of oxygen. Nitrogen oxides (NO_x) emissions were found to be increasing with an increase in adiabatic flame temperature.

Khalil *et al.* [11] investigated the combustion emissions of gaseous fuel using a cylindrical swirl combustor generated through tangential air injection. The emissions of methane and nitrogen-diluted methane mixture were compared. The results showed that addition of nitrogen to the methane decreases NO_x. CO emission showed an increase due to lower flame temperature and decrease in residence time for complete oxidation into carbon dioxide (CO_2). Reddy *et al.* [12] utilised the exhaust gas recirculation concept to reduce the thermal NO_x for biodiesel, 50% biodiesel/diesel swirl flame in a swirl burner. It was reported that the blending of biodiesel with fossil fuel helped in emissions reduction.

The geometry of the burner and swirler also affects the emissions. Bhoi and Channiwala [13] measured the emissions of a 150 kW producer gas-fired premixed burner. The result shows that NO_x emissions increase with swirl angle while CO emissions are independent of swirl angle. The effect of fuel equivalence ratio (ϕ) on emissions was performed by Mafra *et al.* [14] using a liquefied petroleum gas-fired chamber. NO emissions were found to decrease with decrease of fuel ϕ.

Detailed characterisation of a burner can yield valuable insights on the mechanism of flame evolution and flow-flame interactions. In the present paper, a swirl burner is utilised to establish a propane/air premixed flame over a range of equivalence ratio. The non-reacting and reacting conditions of the premixed swirl burner are characterised at atmospheric conditions. The general flame characteristics such as the lean blowout limit, global flame pattern and burning intensity are investigated. The data generated can be used for numerical model validation.

2.0 EXPERIMENTAL AND METHOD

2.1 Burner and Flow Delivery System

The swirl burner used in this experiment consists of an axial swirler and a circular quartz tube placed at the burner outlet. The swirler consists of six straight swirl vanes with a thickness of 1.5 mm. The swirler vanes are fixed at the angle of 45° from the axial centreline axis. The six vanes are equally spaced at 60° around the central swirler hub. The geometrical swirl number, S_N is based on the following equation [15]:

$$S_N = \frac{2}{3}\left[\frac{1-(D_h/D_s)^3}{1-(D_h/D_s)^2}\right]\tan\theta \quad (1)$$

where D_h and D_s represent the swirler hub diameter and the swirler diameter respectively, and θ is the vane angle orientation from the centreline axis. Detailed geometry of the swirler is shown in Figure. 1. The present swirler number is 0.8, which is sufficiently strong to create a stable flame. The strong swirl enables the formation of recirculation zone that recirculates hot products and assists in flame stabilisation [16].

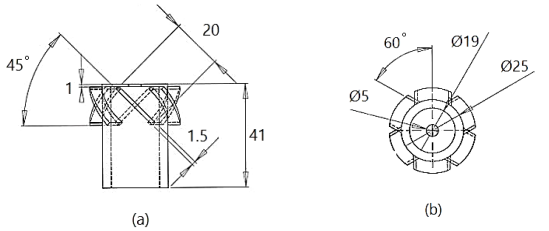

Figure 1 Geometry of the axial swirler (a) front view (b) plan view. Dimensions are in milimetres.

A quartz tube with an internal diameter of 112 mm and length of 400 mm was placed at the burner outlet to form a combustor wall. The quartz tube is able to withstand high temperatures of up to 1100°C, apart from providing visual access to the flames. The main air flow and gaseous fuel were supplied and regulated by two Sierra mass flow controllers (Air: model C50M, Propane: model C50L), which deliver full scale accuracy of ±1% respectively. The mixing of air and fuel occurs at the burner plenum prior to passing through the swirler and entering the combustion chamber. The mixture was ignited using a flame torch at the burner outlet. The schematic of the burner and flow delivery system is shown in Figure. 2.

2.2 Gaseous Fuel

The fuel used in the present experiment is propane (Megamount: 99.5% purity). The propane gas was supplied to the burner plenum at room temperature of 25°C. The properties of the fuel are shown in Table 1.

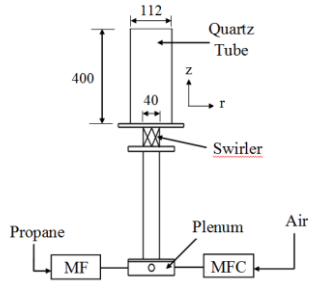

Figure 2 Schematic of flow delivery system. Dimensions are in milimetres.

Table 1 Propane properties.

Properties	Propane
Molecular formula	C_3H_8
Density (kg/m3), 21.1° C	1.83
Flash point (°C)	-104
Autoignition temperature (°C)	540
Heat capacity C_p, (Cal/g)	0.39
Std. enthalpy of combustion (MJ/mol)	-2.22
Vapor pressure (kPa), 21.1° C	853.16
Kinematic viscocity (Ns/m^2), 27° C	1.1 x 10^4

2.3 Operating Conditions

2.3.1 Main Air Flow Velocity

The flow velocity at the burner outlet (z = 0 mm) was measured using a manometer with pitot tube under non-reacting flow condition. The axial air velocity (z-direction) and the bulk magnitude velocity of the flow exiting the swirler (45° parallel to the swirler vane) were measured at the burner outlet for the main air supplies of 0.97, 1.95, 2.92 and 3.90 g/s at room temperature of 25°C.

2.3.2 Flame Imaging

The premixed flame images were taken using a digital single-lens reflex camera (Canon: EOS 5D) at an equivalence ratio range of ϕ = 0.7 – 1.1 under reacting conditions. The effect of main axial air flow rate on the flame was investigated by varying the flow rate between 1.95 to 3.12 g/s to qualitatively observe the characteristics of premixed swirl flames.

2.3.3 Lean Flame Blowout

The burner blowout limit was determined by setting the main air mass flow rate constant at ϕ= 0.8, and reducing the fuel mass flow rate in steps until the flame blows out. The final fuel flow rate at the instant where flame blowout occurs was recorded and the blowout equivalence ratio was determined. The tests were conducted at the main air flow rate of 1.17 - 3.90 g/s at the interval of 0.19 g/s.

2.3.4 Emission Measurements

The post-combustion emissions were examined using a gas analyser (EMS 5002). A sampling probe was placed at the centerline outlet of the quartz tube at z = -42 mm and 400 mm downstream of burner outlet. Equivalence ratio was set at ϕ= 0.7 for axial air supply rate of 1.95 g/s. Emission measurements were

performed at ϕ = 0.7, 0.8, 0.9, 1.0 and 1.1 by adjusting the fuel flow rate accordingly. The procedure was repeated for the main air supply rate of 2.34, 2.73 and 3.12 g/s.

The combustion emission data were recorded when the readings become stabilised (t ~ 1 min). The resolutions for the emission analyser gases are, unburned hydrocarbons (UHCs): 1 ppm vol, carbon monoxide (CO): 0.01 ppm, carbon dioxide (CO_2): 0.1% vol, oxygen (O_2): 0.01% vol and nitrogen oxides (NO_x): 1 ppm. The emissions of the seven spatial points at the interval of 14 mm across the centreline of the burner outlet were measured and averaged to obtain the final emission value. The operating conditions for the tests conducted are shown in Table 2.

Table 2 Operating conditions.

Tests	Air flow rate (g/s)*	Propane flow rate (g/s)	Equivalence ratio □
	Non-reacting		
Air velocity	0.97: 0.97: 3.90	N/A	N/A
	Reacting		
Flame imaging	1.95:0.39:3.12	0.09-0.22	0.7-1.1
Lean blowout limit	1.17:0.19:3.90	< 0.20	< 0.8
Emissions	2.34:0.39:3.12	0.11-0.22	0.7-1.1

* For air flow rate: a:b:c, a = minimum flow rate, b = incremental step, c = maximum flow rate.

■3.0 RESULTS AND DISCUSSION

3.1 Flow Velocities At Burner Outlet

At open (without quartz tube) and non-reacting conditions, the main air flow velocity at axial (z-direction) direction was measured. The flow profile across the dump plane burner outlet (swirl exit) is symmetric, as shown in Figure. 3. The centerline of the burner is marked by the radial position of r = 0 mm. The main air flow exits the swirler at the region between r = 12-20 mm while the bluff body region (r = -10 – 10 mm) shows no axial flow. The highest mean air velocity measured at the burner outlet were 8.3, 6.4, 4.3 and 2.1 m/s for the supplied air flow rate of 3.90, 2.92, 1.95 and 0.97 g/s, respectively.

The magnitude air velocities parallel to the swirl vane angle of 45° were measured to be slightly higher than the axial air velocities by ~2 m/s at the same supplied air flow rate, as shown in Figure. 4. The measured magnitude of air velocities at the burner outlet were 9.6, 7.6, 5.4 and 2.9 m/s for the main air flow rate of 3.90, 2.92, 1.95 and 0.97 g/s, respectively. The higher magnitude velocity at the burner outlet was split into the axial and tangential components. The flow profile at downstream of combustor wall outlet (z = 40 mm) is shown in Figure. 5. The flow profile peaks at the centreline of the burner wall exit and gradually decreases near the wall due to boundary layer effects.

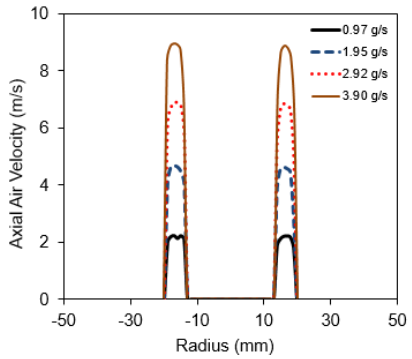

Figure 3 Axial air velocity across burner outlet.

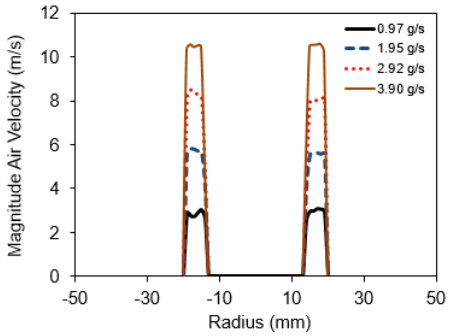

Figure 4 Magnitude air velocity across burner outlet.

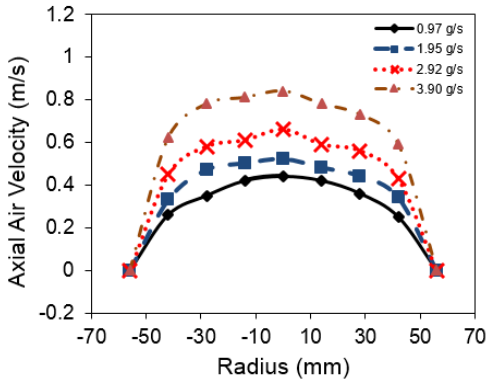

Figure 5 Axial air velocity across quartz tube outlet.

3.2 Global Flame Imaging

The flame shape and intensity at a range of equivalence ratios are shown in Figure. 6. Premixed swirl flame results in a short and compact flame, stabilizing near the burner outlet. At lean-burning condition (ϕ = 0.7), the flame shows a pale bluish flame, with some degree of instability and susceptible to blowout. As the equivalence ratio increases to ϕ = 0.8, the flame becomes more intense and stable. The flame stabilises at the burner outlet with a slight reduction in flame height. At ϕ = 0.9, the flame becomes even more stable with increased intensity. Some reddish flame downstream of the main reaction zone was observed.

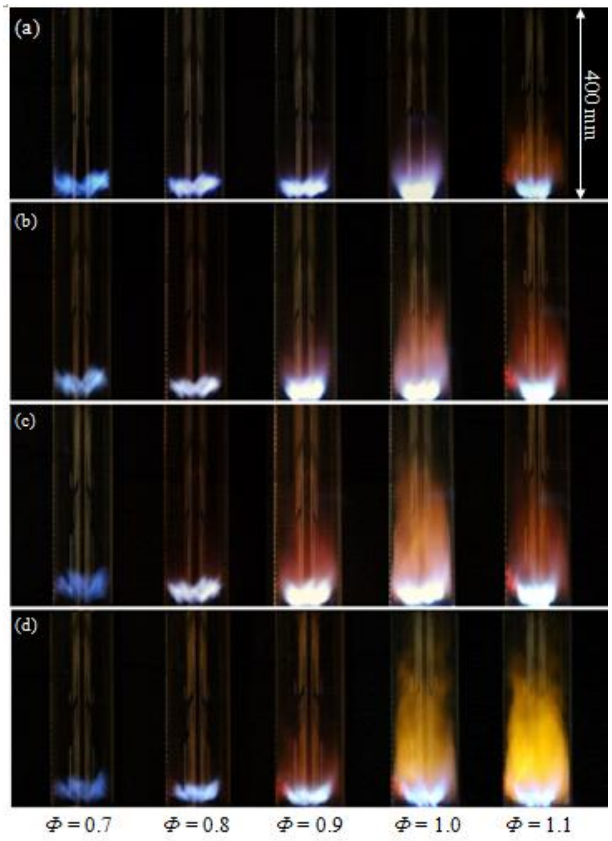

Figure 6 Flame images at different equivalence ratio for main air flow rate of (a) 1.95 (b) 2.34 (c) 2.73 and (d) 3.12 g/s.

Further increase in equivalence ratio results in the increased flame burning intensity. At rich-burning region ($\phi > 1$), the flame primary reaction zone turns into intense white-bluish flame, in addition to the increase of reddish post-reaction flame. The presence of reddish-orange post flame indicates the inclination of the flame to produce soot as a result of incomplete combustion.

The effects of the main air supply on the flame shape and intensity for the range of equivalence ratios are compared qualitatively via images as shown in Figures 6a-d. As the main air mass flow rate is increased from 1.95 to 3.12 g/s, there is a visible increase of flame intensity near stoichiometry and in the rich-burning regions. This is attributed to the corresponding increase in fuel mass flow rate and power output. The high swirl of the burner promotes mixing and reactions. For lean-burning region of $\phi \leq 0.8$, flame intensity is relatively weaker due to the low heat release rate. The established premixed at $\phi \leq 0.7$ shows the flame root is not attached to the burner outlet, hence susceptible to flame blowout.

3.3 Blowout Limit

The lean blowout limit was determined as a function of main air flow rate as shown in Figure 7. The plots indicate the equivalence ratio at which flame blowout occured. The region above the plot indicates the stable swirl flame region. In general, the flame can be established at $\phi > 0.5$ for the air mass flow rates ranging 1.56-3.90 g/s, indicating stable operating regime. For air flow supply rate less than 1.56 g/s, insufficient air flow results in weak swirl and recirculation flow within the combustor. This affects the flame as the high temperature product post reaction zone is not able to recirculate back to the burner outlet to assist in flame stabilisation, thus resulting in flame blowout at higher equivalence ratio.

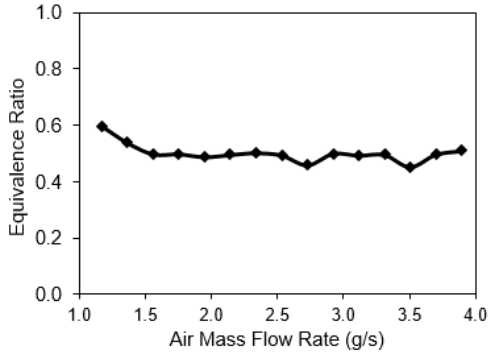

Figure 7 The equivalence ratio at which lean blowout occurs at different air mass flow rate.

3.4 Emission Performance

3.4.1 Nitrogen Oxides

Emissions variation of NO_x for premixed propane/air mixture as a function of equivalence ratio and main air mass flow rate are shown in Figure. 8. In general, NO_x emissions are less than 10 ppm at $\phi = 0.7$, but increases with equivalence ratio before peaking at stoichiometric condition. NO_x emission is reduced by 48% at $\phi = 1.1$ as compared to $\phi = 1.0$. Variations of the main air and fuel mass flow rate show similar trend, despite differences in emissions values. The differences in NO_x emission are more obvious in the stoichiometric and rich-burning regions.

NO_x emissions is highly dependent on the flame temperature, where thermal NO_x is prone to form at high temperature, as explained by the Zeldovich mechanism [17]. As the equivalence ratio of the mixture is close to stoichiometry, the temperature of flame increases with increased supply of fuel, resulting in the formation of NO_x. Similar NO_x emission trend was reported by Alasfour [18] in an experiment using butanol as fuel. NO_x emissions increase from $\phi = 0.75$ and reach a peak at about $\phi = 0.9$, before dropping at equivalence ratio of 1 until 1.05. The lower NO_x emission on the rich-burning region is due to the decomposition of NO_x more than the reduced formation of NO_x [19].

3.4.2 Carbon Monoxides

The emission of CO is not noticeable at lean premixed-burning conditions but becomes obvious at stoichiometric and rich-burning region, as shown in Figure. 9. The overall average value is within 2 ppm for the range of equivalence ratios and main air flow rates tested. The highest average CO emission value is 1.84 ppm under rich-burning of $\phi = 1.1$ for the air flow rate of 2.34 g/s. The low value of CO emission indicates complete combustion under premixed combustion mode and sufficient residence time for CO to be converted to CO_2 in the long quartz tube (400 mm).

3.4.3 Unburned Hydrocarbons

Unburned hydrocarbons emissions are generally low (< 10 ppm) for all equivalence ratios and main air flow rates tested as shown in Figure 10. The highest average UHCs emission is 8 ppm at the equivalence ratio of $\phi = 0.7$ when the main air flow rate is set at 3.12 g/s. Emission of UHCs is not clearly evident (< 2 ppm) at

rich-burning conditions, i.e. ϕ=1.1, possibly due to sufficient time for UHCs from the sooty flame to be oxidised within the combustor.

3.4.4 Carbon Dioxides

The CO_2 emission value increases with equivalence ratio for all range of air flow rates as shown in Figure 11. A slight drop of CO_2 was observed at ϕ = 1.1 as compared to ϕ = 1.0. The slightly higher CO_2 for flow rate of 2.73 and 3.12 g/s could be due to the increased fuel mass flow and complete CO conversion into CO_2.

3.4.5 Oxygen

Overall, the average values of O_2 emitted drop with the increase in equivalence ratio for all flow rates as shown in Figure12. This trend is the inverse to that of CO_2 as oxygen is used in the oxidation process by CO to form CO_2. The oxidation process of CO undergoes the equation $CO + O_2 \rightarrow CO_2 + O$ [20]. A slight increase of oxygen was observed at equivalence ratio ϕ = 0.9 at the main air flow rate 1.95 g/s, possibly due to the flow field effect within the combustor.

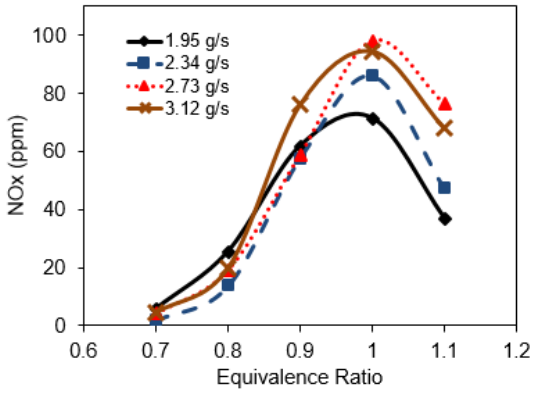

Figure 8 Emissions of NO_x as a function of equivalence ratio operating at different main air flow rates.

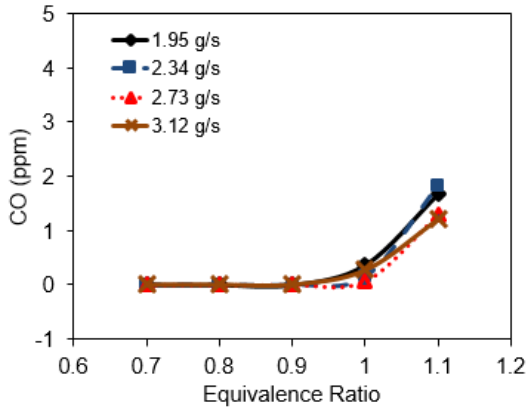

Figure 9 Emissions of CO as a function of equivalence ratio operating at different main air flow rates.

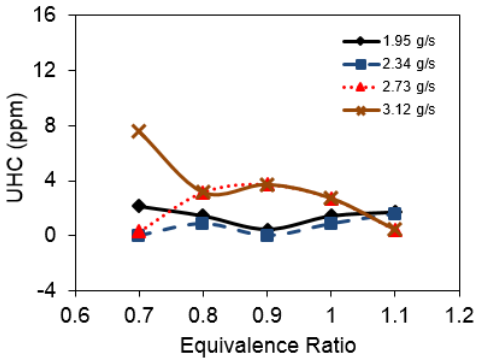

Figure 10 Emissions of unburned hydrocarbon as a function of equivalence ratio operating at different main air flow rates.

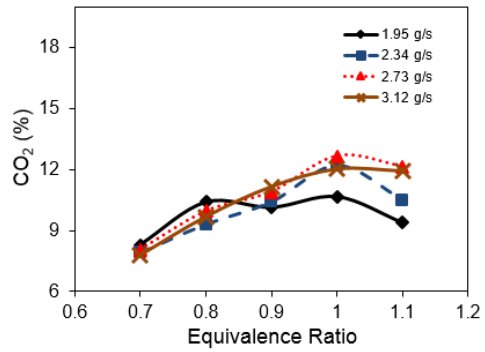

Figure 11 Emissions of carbon dioxides as a function of equivalence operating different main air flow rates.

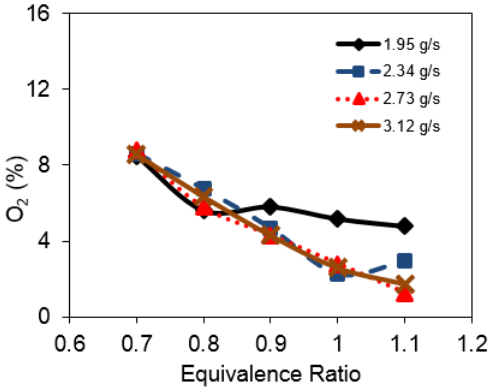

Figure 12 Emissions of oxygen as a function of equivalence ratio operating different main air flow rates.

4.0 CONCLUSION

Characterisation of a premixed swirl burner has been performed under non-reacting and reacting conditions. The air velocities from the burner outlet were measured under non-reacting condition. Images of the premixed flames over a range of equivalence ratios show the flame shape and intensity qualitatively. The lean blowout limit was determined to map the operating regime of the burner. Emissions of the premixed propane/air mixtures show that NO_x peaks at stoichiometric

condition where the flame temperature is the highest. CO and UHCs emissions are generally low for premixed flames.

Acknowledgement

The financial support from the Ministry of Higher Education (MOHE) Malaysia and Universiti Teknologi Malaysia (Research university grant vot number: 06H29) is gratefully acknowledged.

References

[1] N.A. Chigier and A. Chervinsky. 1967. Aerodynamic study of turbulent burning free jets with swirl. *Symposium (International) on Combustion.* 11(1): 489–499.
[2] X. Jiang, K.H. Luo, L.P.H. de Goey, R.J.M. Bastiaans, and J.A.V. Oijen. 2011. Swirling and impinging effects in an annular nonpremixed jet flame. *Flow turbulence combustion* .86(1): 63–88.
[3] Z.H. Chen, G.E. Liu, and S.H. Sohrab. 1987. Premixed flames in counterflow jets under rigid-body rotation. *Combustion Science and Technology.* 51(1–3): 39–50.
[4] A.E.E. Khalil and A.K. Gupta. 2013. Fuel flexible distributed combustion for efficient and clean gas turbine engines. *Applied energy.* 109: 267–274.
[5] C. T. Chong and S. Hochgreb. 2013. Flow field of a model gas turbine swirl burner. *Advanced Materials Research.* 622: 1119–1124.
[6] C.T. Chong and S. Hochgreb. 2012. Spray combustion characteristics of palm biodiesel. *Combustion Science and Technology.* 184(7-8): 1093–1107.
[7] C.T. Chong and S. Hochgreb. 2014. Spray flame structure of rapeseed biodiesel and Jet-A1 fuel. *Fuel.* 115: 551–558.
[8] C.T. Chong and S. Hochgreb. 2013. Spray flame study using a model gas turbine swirl burner. *Applied Mechanics and Materials* 316–317:17–22.
[9] M.A. Nemitallah and M.A. Habib. 2013. Experimental and numerical investigations of an atmospheric diffusion oxy-combustion flame in a gas turbine model combustor. *Applied energy.* 111:401–415.
[10] H.S. Kim, V.K. Arghode, M.B. Linck, and A.K. Gupta. 2009. Hydrogen addition effects in a confined swirl-stabilized methane-air flame. *International Journal of Hydrogen Energy.* 34 (2): 1054–1062.
[11] A.E.E. Khalil, V.K. Arghode, A.K. Gupta, and S. C. Lee. 2012. Low calorific value fuelled distributed combustion with swirl for gas turbine applications. *Applied energy.* 98:69–78.
[12] V.M. Reddy, P. Biswas, P. Garg, and S. Kumar. 2014. Combustion characteristics of biodiesel fuel in high recirculation conditions. *Fuel Processing Technology.* 118:310–17.
[13] P.R. Bhoi and S. A. Channiwala. 2009. Emission characteristics and axial flame temperature distribuion of producer gas fired premixed burner. *Biomass and Bioenergy.* 33(3): 469–477.
[14] M.R. Mafra, F. L. Fassani, E. F. Zanoelo, and W. A. Bizzo. 2010. Influence of swirl number and fuel equivalence ratio on NO emission in an experimental LPG-fired chamber. *Applied Thermal Engineering.* 30(8–9): 928–934.
[15] J.M. Beer and N.A. Chigier. 1972. Combustion aerodynamics, *Appl. Sci. Publ. London.*
[16] V. Tangirala, R. H. Chen, and J. F. Driscoll. 1987. Effect of heat release and swirl on the recirculatioin within swirl-stabilized flames. *Combust. Sci. Technol.* 51:75–95.
[17] C.P. Fenimore. 1979. Studies of fuel-nitrogen species in rich flame gases. *Symposium (International) on Combustion.* 17(1): 661–670.
[18] F.N. Alasfour. 1998. NOx emission from a spark ignition engine using 30% iso-butanol-gasoline blend: part 2-ignition timing. *Applied Thermal Engineering.* 18(8): 609–618.
[19] M. Watfa and H. Daneshyar. 1975. Formation of nitric oxide (NO), carbon monoxide (CO) and unburnt hydrocarbons (HC) in spark ignition engines. *IMechE, Combustion in Engines Conference, Cranfield CP6-C9975*
[20] I. Glassman, 1996. *Combustion.* 3rd ed. California, USA: Academic Press.